Computational Study of B_4H_{10} Addition to Ethene. Baskets from Boranes[†]

Michael Bühl*

Organisch-chemisches Institut, Universität Zürich, Winterthurerstrasse 190,
CH-8057, Zürich, Switzerland

Michael L. McKee*

Department of Chemistry, Auburn University, Auburn, Alabama 36849

Received March 27, 1998

Three pathways leading from $B_4H_{10} + C_2H_4$ to $(CH_2CH_2)B_4H_8$ are examined at the [MP4/6-311+G(d,p)]//MP2/6-31G(d) + ZPC level. The preferred, "addition" path involves transient $[B_4H_8]$, $[B_4H_8(C_2H_4)]$, and a cage-opened $[(CH_2CH_2)B_4H_8]$ intermediate with a rate-determining barrier of 33.0 kcal/mol (for $[B_4H_8]$ formation). "Indirect hydroboration" of ethene via $[B_4H_8]$ is disfavored by entropy and can be excluded. "Direct hydroboration" via a higher-energy $[B_4H_{10}]$ isomer can be competitive; the overall energetic barrier for this process is only 26.9 kcal/mol, but the hydroboration step is disfavored by entropy to such an extent that the "addition" path is the main route at the experimental temperatures. Direct hydroboration affords the intermediate $Et-B_4H_9$ which is likely to be involved in side reactions leading to byproducts such as $Et-(CH_2CH_2)B_4H_7$.

Introduction

Mechanistic studies of carborane formation have been a continuing field of study.[1−6] Reactions of unsaturated compounds, such as alkynes and alkenes, with boron hydrides often produce a surprising mixture of compounds in ratios that vary with reaction conditions. In addition, if deuterium or ^{11}B is incorporated into the starting material, the label is often scrambled in the products.[7,8] The evidence indicates that carborane formation may involve a number of competing pathways, involving addition, elimination, and rearrangement.

$$\underset{\mathbf{2}}{B_4H_{10}} + C_2H_4 \rightarrow \underset{\mathbf{1}}{(CH_2CH_2)B_4H_8} + H_2 \qquad (1)$$

The formation of $(CH_2CH_2)B_4H_8$ (**1**) according to eq 1 is one of the more interesting carborane reactions[9−15] in that it vindicates one of the earliest structural predictions for the product of the acetylene/boron hydride reaction, i.e., that the boron hydride simply adds a carbon−carbon handle.[3] Only later was it realized that both carbons adopted vertex positions.[3] Thus, the "basketlike" structure of $(CH_2CH_2)B_4H_8$ (see Figure 1 below) gives a sense of *déjà vu* and proves that boron hydrides with handles can exist.[3]

In the pyrolysis of B_4H_{10} (**2**), added H_2 dramatically decreases the rate of thermolysis while leaving the activation barrier unaltered.[16] This suggests that the first step in the reaction is the elimination of H_2 (eq 2a).

$$\underset{\mathbf{2}}{B_4H_{10}} \rightarrow \underset{\mathbf{3}}{B_4H_8} + H_2 \qquad (2a)$$

[†] Dedicated to Heinrich Nöth on the occasion of his 70th birthday.

(1) Grimes, R. N. *Carboranes*, Academic Press: New York, 1970; pp 23−31.
(2) Williams, R. E. *Chem. Rev.* **1992**, *92*, 177.
(3) For an excellent review, see: Williams, R. E. Early Carboranes and Their Structural Legacy. In *Advances in Organometallic Chemistry*; Stone, F. G. A., West, R., Eds.; Academic Press: New York, 1994; Vol. 36, pp 1−55.
(4) (a) McKee, M. L. *J. Am. Chem. Soc.* **1995**, *117*, 8001. (b) McKee, M. L. *J. Am. Chem. Soc.* **1996**, *118*, 421.
(5) (a) McKee, M. L. Fluxional Processes in Boranes and Carboranes. In *The Encyclopedia of Computational Chemistry*; Allinger, N. L., Clark, T., Gasteiger, J., Kollman, P. A., Schaefer, H. F., Schleyer, P. v. R., Eds., Wiley: New York, in press. (b) McKee, M. L. "Mechanistic Patterns in Carborane Reactions. In *The Borane, Carborane and Carbocation Continuum*; Casanova, J., Ed.; Wiley: New York, 1998.
(6) Fox, M. A.; Greatrex, R.; Nikrahi, A.; Brain, P. T.; Picton, M. J.; Rankin, D. W. H.; Robertson, H. E.; Bühl, M.; Li, L.; Beaudet, R. A. *Inorg. Chem.* **1998**, *37*, 2166.
(7) Gaines, D. F.; Coons, D. E.; Heppert, J. A. The Elucidation of Cluster Rearrangement Mechanisms Using Isotopically Labeled Boron Hydrides. In *Molecular Structure and Energetics. Advances in Boron and the Boranes*; Liebman, J. F., Greenberg, A. G., Williams, R. E., Eds.; VCH: New York, 1988; p 91.
(8) Gaines, D. F. In *Boron Chemistry, Proceedings of the 6th International Meeting on Boron Chemistry (IMEBORON)*; Hermánek, S., Ed.; World Scientific: Singapore, 1987; p 118.
(9) Harrison, B. C.; Solomon, I. J.; Hites, R. D.; Klein, M. J. *J. Inorg. Nucl. Chem.* **1960**, *14*, 195.
(10) Shapiro, I.; Williams, R. E.; Gibbins, S. G. *J. Phys. Chem.* **1961**, *65*, 1061.
(11) Williams, R. E.; Gerhart, F. J. *J. Organomet. Chem.* **1967**, *10*. 168.
(12) (a) Onak, T.; Gross, K.; Tse, J.; Howard, J. *J. Chem. Soc., Dalton Trans.* **1973**, 2633. (b) Cranson, S. J.; Fox, M. A.; Greatrex, R.; Greenwood, N. N. *J. Organomet. Chem.* **1998**, *550*, 207.
(13) Hnyk, D.; Brain, P. T.; Rankin, D. W. H.; Robertson, H. E.; Greatrex, R.; Greenwood, N. N.; Kirk, M.; Bühl, M.; Schleyer, P. v. R. *Inorg. Chem.* **1994**, *33*, 2572.
(14) Brain, P. T.; Bühl, M.; Fox, M. A.; Greatrex, R.; Leuschner, E.; Picton, M. J.; Rankin, D. W. H.; Robertson, H. E. *Inorg. Chem.* **1995**, *34*, 2841.
(15) Brain, P. T.; Bühl, M.; Fox, M. A.; Greatrex, R.; Hnyk, D.; Nikrahi, A.; Rankin, D. W. H.; Robertson, H. E. *J. Mol. Struct*. **1998**, *445*, 319.
(16) (a) Greenwood, N. N. In *Electron Deficient Boron and Carbon Clusters*; Olah, G. A., Wade, K., Williams, R. E., Eds.; Wiley: New York, 1991; p 165. (b) Greatrex, R.; Greenwood, N. N.; Potter, C. D. *J. Chem. Soc., Dalton Trans.* **1984**, 2435. (c) Greatrex, R.; Greenwood, N. N.; Potter, C. D. *J. Chem. Soc., Dalton Trans.* **1986**, 81.

S0020-1669(98)00352-8 CCC: $15.00

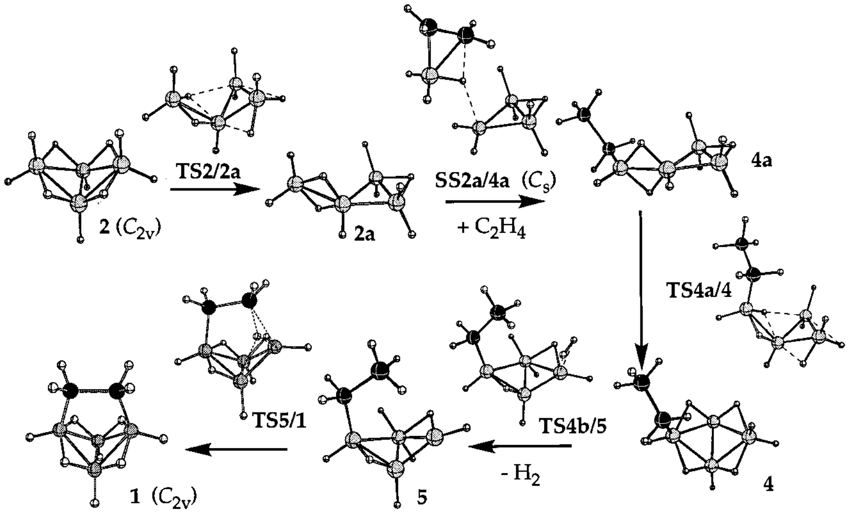

Figure 1. Stationary points along path I, MP2/6-31G(d) optimized.

It is also reasonable to assume that formation of B_4H_8 (**3**) might be the first step in the reaction of **2** with C_2H_4 which is then followed by eq 2b.

$$\mathbf{3} + C_2H_4 \rightarrow \mathbf{1} \qquad (2b)$$

However, a very recent example by Fox et al.[17] demonstrates that **2** can react with an unsaturated hydrocarbon (allene) to form an addition product *without* the loss of H_2 (eq 3). Thus, in the formation of **1** according to eq 1, direct hydroboration with **2** may be competitive with the two-step process (eqs 2a + 2b).

$$B_4H_{10} + H_2C{=}C{=}CH_2 \rightarrow (MeCHCH_2)B_4H_8 \qquad (3)$$

Another possible example of direct hydroboration may be found in the reaction of **2** with $H_2C{=}CHCH_3$.[14] One of the minor products is a propyl-substituted basket, Pr−($MeCHCH_2$)-B_4H_8. A possible path would be eq 4a or 4b followed by eq 5.

$$B_4H_{10} \xrightarrow{+C_3H_6} Pr{-}B_4H_9 \xrightarrow{-H_2} Pr{-}B_4H_7 \qquad (4a)$$

$$B_4H_{10} \xrightarrow{-H_2} B_4H_8 \xrightarrow{+C_3H_6} Pr{-}B_4H_7 \qquad (4b)$$

$$Pr{-}B_4H_7 + C_3H_6 \rightarrow Pr{-}(MeCHCH_2)B_4H_7 \qquad (5)$$

Since $(MeCHCH_2)B_4H_8$ does not react with propene,[14] the propyl substituent must be incorporated before the basket is formed.

Another example of B_4H_{10} reactivity is the reaction between B_4H_{10} and $H_2C{=}CHC{\equiv}CH$.[18] The major products share a pentagonal pyramid structure with either three or four carbon vertexes. Three of the products involve the complete cleavage of the carbon−carbon triple bond, and in one, the last carbon (with attached substitutent) has been eliminated. Needless to say, the reaction surface is likely to be very complicated.

Hydroboration[19] of ethene by a borane is expected to produce an ethylborane (eqs 6−9).

$$C_2H_4 + BH_3 \rightarrow Et\text{-}BH_2 \qquad (6)$$

$$C_2H_4 + B_4H_{10} \rightarrow \underset{\mathbf{4}}{Et\text{-}B_4H_9} \qquad (7)$$

$$C_2H_4 + B_4H_8 \rightarrow \underset{\mathbf{5}}{Et\text{-}B_4H_7} \qquad (8)$$

$$C_2H_4 + B_5H_9 \rightarrow Et\text{-}B_5H_8 \qquad (9)$$

While ethyltetraborane(10) (**4**) is not known, 1-ethylpentaborane(9) is well characterized.[20] Pyrolysis of 1-ethylpentaborane at 500 °C gives a mixture of carborane products including 2-Me−2-CB_5H_8, which indicates that an alkyl group can be incorporated into a carborane cage.[20] While the mechanism is not known, initial loss of H_2 (eq 10) is plausible.

$$1\text{-}Et{-}B_5H_8 \xrightarrow{-H_2} \rightarrow \rightarrow 2\text{-}Me{-}2\text{-}CB_5H_8 \qquad (10)$$

The analogous mechanism for B_4H_{10} is given in eq 11 where the supposed reaction stops after the first hydroboration.

$$2\text{-}Et{-}B_4H_9 \xrightarrow{-H_2} \rightarrow 2\text{-}Et{-}B_4H_7 \rightarrow (CH_2CH_2)B_4H_8 \qquad (11)$$

It is noteworthy that the reaction of B_4H_8CO with C_2H_4 also gives the basket compound **1**.[12] Since B_4H_8CO generally reacts by eliminating CO, the formation of the basket is consistent with addition of C_2H_4 to **3**.

Williams and Gerhart[11] carried out a key experiment on the mechanism of formation of **1** when they reacted **2** with C_2D_4. If hydroboration were the first step, then one would expect some loss of deuterium in the product (Scheme 1, path I), provided at least one of the eliminated H atoms originates from the Me group of intermediate **4**.

If C_2D_4 adds to **3** (after loss of H_2 from **2**), then all four deuteriums would be found in the product, regardless of the nature of further intermediates that might be involved (paths II and III). Williams' and Gerhart's results argued against path I

---

[17] Fox, M. A.; Greatrex, R.; Hofmann, M.; Schleyer, P. v. R.; Williams, R. E. *Angew. Chem., Int. Ed. Engl.* **1997**, *36*, 1498.

[18] Fox, M. A.; Greatrex, R.; Nikrahi, A. *Chem. Commun.* **1996**, 175.

[19] Brown, H. C. *Hydroboration*; Benjamin: New York, 1962.

[20] Groszek, E.; Leach, J. B.; Wong, G. T. F.; Ungermann, C.; Onak, T. *Inorg. Chem.* **1971**, *10*, 2770.

Scheme 1

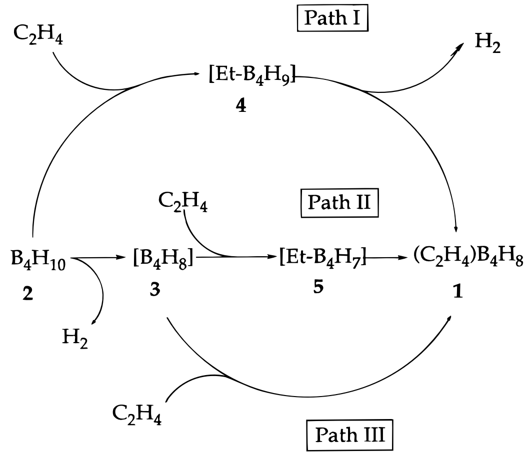

because their mass-spectrometric analysis showed all four deuteriums incorporated into the product.

In the case of hydroboration of C_2D_4 by **3** (path II), the resulting intermediate would possess a $-CD_2CD_2H$ group, and one would expect the final basket d_4-**1** to contain an appreciable fraction of H atoms in the handle. However, the experimental infrared spectra[11] showed the absence of any CH stretching frequencies in d_4-**1**, suggesting a route via direct addition of ethene to **3** (path III). However, a competition between path II and path III cannot be eliminated since a small amount of product with CH substitution might have escaped detection.

We report herein a computational comparison of the three pathways, I, II, and III.

Computational Methods

All geometries were fully optimized in the given symmetry at the MP2/6-31G(d) level.[21] Vibrational frequencies were calculated at that level to determine the nature of the stationary points and to make zero-point corrections (frequencies weighted by a 0.95 factor). Single-point calculations were performed at the MP4/6-31G(d) and MP2/6-311+G-(d,p) levels and combined[22] to estimate relative energies at the [MP4/6-311+G(d,p)] level, which, when zero-point corrections have been added, will constitute the "standard" level. All MP2 and MP4 calculations were made with the "frozen-core" approximation.

Heat capacities and entropy corrections were made using unscaled frequencies and standard statistical procedures[23] to determine relative enthalpies and free energies at 298 and 373 K.

The MP2/6-31G(d) method has been shown to yield accurate geometries for boranes and carboranes.[24] Mechanistic aspects of carborane formation have been investigated previously using the same methodology as employed here.[4,5]

Molecular plots of the relevant structures are given in Figures 1−3 (C_1 symmetry except where otherwise noted). A table of total energies (hartrees) and zero-point energies (kcal/mol) as well as Cartesian coordinates of all species are provided as Supporting Information.

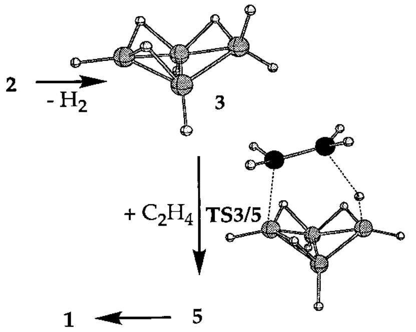

Figure 2. Stationary points along path II, MP2/6-31G(d) optimized.

A boldface notation system is used for the species in the figures, tables, and text to aid in identification. For example, the bold notation **TSx/y** refers to the transition state between structures **x** and **y** (which may also involve other reaction partners). Relative energies, enthalpies, and free energies (kcal/mol) are presented in Table 1 with respect to the top entry in each section of structures. A potential-energy diagram of computed energies ("standard level") is given in Figure 4 for the various reaction pathways from **2** + C_2H_4 to the products **1** + H_2.

Results and Discussion

We have started our investigation with the addition of BH_3 to C_2H_4, a reaction which has been studied previously both experimentally[25] and theoretically.[26,27]

We calculate a π-complex for the BH_3 addition to C_2H_4 which is 7.8 kcal/mol more stable than reactants (Table 1). However, the existence of the π-complex on the potential energy surface is called into question, because, with corrections, the transition state (**TS(BH_3 + C_2H_4)**) is 0.1 kcal/mol *more stable* than the π-complex. Nevertheless, including heat capacity and entropy effects for **TS(BH_3 + C_2H_4)** gives a free energy barrier (298K) of 2.4 kcal/mol which compares very well to the reported free energy of activation of 2 ± 3 kcal/mol.[25] At the QCISD(T)/6-311+G**//QCISD/6-31G* level of theory,[27] a π-complex is predicted on the PES with a very small barrier (0.05 kcal/mol) for formation of ethylborane.

If attention is turned to the **2** + C_2H_4 reaction, three different mechanisms are considered for formation of the basket compound **1** (Scheme 1). We will call these the following: "direct" hydroboration (path I), "indirect" hydroboration (path II), and "addition" (path III). In path I, **2** itself is the hydroborating agent and in path II **3** is the hydroborating agent, while, in path III, C_2H_4 adds to **3**.

Direct Hydroboration (Path I). The first step in direct hydroboration is the rearrangement of B_4H_{10} (**2**) to a higher-energy isomer (**2a**) via a transition state (**TS2/2a**) with a 26.9 kcal/mol activation energy (Figure 1). The intermediate **2a**, 10.4 kcal/mol less stable than **2**, can be viewed as two diboranes fused together through the elimination of one terminal and one bridging hydrogen. The pentacoordinate boron in **2a** has some similarity to a higher-energy isomer of B_3H_9, which has been suggested to be involved in diborane pyrolysis.[28]

Ethene can add to **2a** with an activation barrier of 15.1 kcal/mol (**SS2a/4a**) to produce **4a** in a reaction that is 28.9 kcal/mol exothermic (Table 1). At the MP2/6-31G(d) level, **SS2a/4a** is a second-order saddle point (two imaginary frequencies) and

---

(21) Frisch, M. J.; Trucks, G. W.; Schlegel, H. B.; Gill, P. M. W.; Johnson, B. G.; Robb, M. A.; Cheeseman, J. R.; Keith, T.; Petersson, G. A.; Montgomery, J. A.; Raghavachari, K.; Al-Laham, M. A.; Zakrzewski, V. G.; Ortiz, J. V.; Foresman, J. B.; Cioslowski, J.; Stefanov, B. B.; Nanayakkara, A.; Challacombe, M.; Peng, C. Y.; Ayala, P. Y.; Chen, W.; Wong, M. W.; Andres, J. L.; Replogle, E. S.; Gomperts, R.; Martin, R. L.; Fox, D. J.; Binkley, J. S.; Defrees, D. J.; Baker, J.; Stewart, J. P.; Head-Gordon, M.; Gonzalez, C.; Pople, J. A. *Gaussian94*, rev. E.2; Gaussian, Inc.: Pittsburgh, PA, 1995.

(22) (a) McKee, M. L.; Lipscomb, W. N. *J. Am. Chem. Soc.* **1981**, *103*, 4673. (b) Nobes, R. H.; Bouma, W. J.; Radom, L. *Chem. Phys. Lett.* **1982**, *89*, 497. (c) McKee, M. L.; Lipscomb, W. N. *Inorg. Chem.* **1985**, *24*, 762.

(23) McQuarrie, D. A. *Statistical Thermodynamics*; Harper & Row: New York, 1973.

(24) Bühl M.; Schleyer, P. v. R. *J. Am. Chem. Soc.* **1992**, *114*, 477.

(25) Fehlner, T. *J. Am. Chem. Soc.* **1971**, *93*, 6366.

(26) Wang, X.; Li, Y.; Wu, Y.-D.; Paddon-Row: M. N.; Rondan, N. G.; Houk, K. N. *J. Org. Chem.* **1990**, *55*, 2601.

(27) Hommes, N. J. R. v. E.; Schleyer, P. v. R. *J. Org. Chem.* **1991**, *56*, 4074.

(28) Duke, B. J.; Liang, C.; Schaefer, H. F. *J. Am. Chem. Soc.* **1991**, *113*, 2884.

Table 1. Relative Energies, Enthalpies, and Free Energies (kcal/mol) of Various Species[a]

	relative energies						thermodyn values	
	MP2/a	MP4/a	MP2/b	[MP4/b]	+ZPC[b]	Δ*H*(298 K)	Δ*G*(298 K)	Δ*G*(373 K)
$BH_3 + C_2H_4$	0.0	0.0	0.0	0.0	0.0	0.0	0.0	0.0
π-complex	−13.1	−11.3	−13.6	−11.8	−7.8	−8.8	1.5	4.0
TS(BH_3+ C_2H_4)	−13.1	−11.3	−13.6	−11.8	−7.8	−9.3	2.4	5.3
BH_2−Et	−36.2	−34.1	−36.2	−34.0	−28.9	−29.8	−19.6	−17.1
B_4H_{10} (**2**) + C_2H_4	0.0	0.0	0.0	0.0	0.0	0.0	0.0	0.0
TS2/2a + C_2H_4	34.3	32.3	32.0	29.9	26.9	27.7	25.8	25.6
[B_4H_{10}] (**2a**) + C_2H_4	12.8	11.2	12.4	10.8	10.4	11.4	10.0	9.6
TS**2a**/**4a**	26.9	27.2	26.2	26.5	25.5	26.4	33.5	35.3
SS**2a**/**4a**	26.9	27.1	26.3	26.5	25.4	25.7	34.7	36.9
TS (BH_3 + C_2H_4) + B_3H_7	31.5	31.1	32.6	32.2	29.8	29.9	28.3	27.8
Et−B_4H_9] (**4a**)	−22.0	−21.4	−22.8	−22.2	−18.5	−17.6	−9.0	−6.8
TS4a/4	0.1	0.4	−2.5	−2.2	−0.9	−0.9	9.3	11.9
"*gauche*"-Et−B_4H_9 (**4**)	−32.6	−30.4	−32.9	−30.7	−26.5	−26.7	−16.1	−13.4
"*syn*"-Et−B_4H_9 (**4b**)	−31.0	−28.8	−31.5	−29.3	−25.0	−25.3	−14.1	−11.3
TS4b/5	17.4	17.9	14.6	15.1	13.7	13.2	23.0	25.4
Et−B_4H_7 (**5**) + H_2	12.2	12.5	11.8	12.1	8.2	10.1	11.9	12.3
TS5/1 + H_2	22.1	25.8	17.9	21.6	17.9	18.0	22.2	23.3
(CH_2CH_2)B_4H_8 (**1**) + H_2	−19.8	−17.4	−20.8	−18.4	−20.2	−20.0	−15.6	−14.5
TS2/3+ C_2H_4	41.5	39.7	39.2	37.4	33.0	33.4	32.4	32.1
B_4H_8 (**3**) + H_2+C_2H_4	22.2	22.1	23.2	22.1	15.1	16.3	7.3	5.0
TS3/5 + H_2	40.4	42.4	37.8	39.9	34.7	35.2	38.5	39.4
TS3/1 + H_2	43.7	47.7	40.6	44.6	39.5	40.2	43.1	43.8
TS3/1a + H_2	33.3	32.1	34.5	33.3	27.4	28.8	28.0	27.7
$B_4H_8(C_2H_4)$ (**1a**) + H_2	−0.4	3.8	0.7	4.9	2.6	3.3	6.1	6.8
TS1a/1b + H_2	16.9	16.9	16.6	16.6	11.7	12.5	15.3	15.9
[$(C_2H_4)B_4H_8$] (**1b**) + H_2	8.6	8.7	9.4	9.5	4.5	5.9	7.0	8.4
TS1b/1 + H_2	23.4	23.6	20.7	20.9	15.4	16.0	19.2	20.1

[a] Basis set "a" is 6-31G(d); basis "b" is 6-311+G(d,p). [b] Zero-point correction, made with a 0.95 scaling factor.

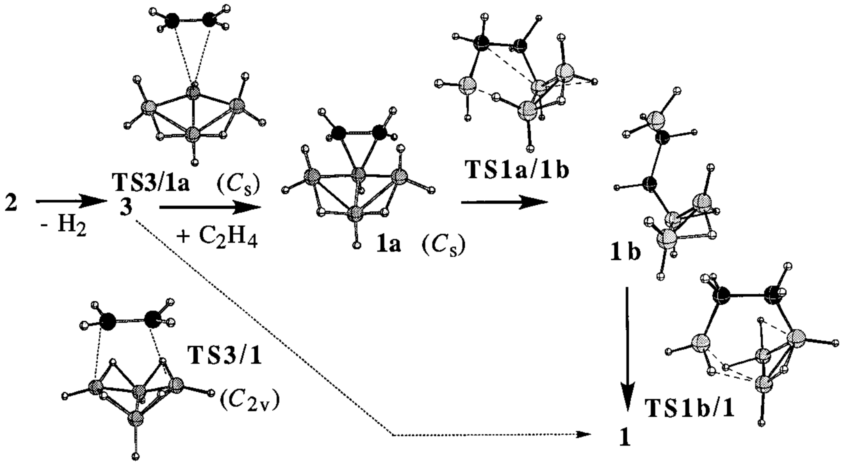

Figure 3. Stationary points along path III, MP2/6-31G(d) optimized.

relaxes to the true transition state (**TS2a/4a**) with loss of the plane of symmetry. However, the energy lowering from **SS2a/4a** to **TS2a/4a** is very small and the energy order reverses with zero-point correction. The transition structure **SS2a/4a** can be best described as a $BH_3 + C_2H_4$ transition state, stabilized through the interaction of the transferring hydrogen with the vacant orbital of a B_3H_7 unit. The energy of **SS2a/4a** is 4.4 kcal/mol lower than **TS(BH_3 + C_2H_4)** plus B_3H_7 (Table 1), which indicates that the stabilization is modest. Thus, if path I is competitive, one might also expect ethylborane as a product. Indeed, in the hot−cold reaction of **2** and C_2H_4, one of the minor products is BEt_3 which could arise from the further reaction of ethylborane with two molecules of ethene.[15]

Intermediate **4a**, an ethyl-substituted version of **2a**, has a 17.6 kcal/mol barrier (**TS4a/4**) to formation of **4**, an ethyl-substituted tetraborane(10). For the reaction to proceed to the basket **1**, H_2 must first be eliminated from **4**; this can occur by a 60° rotation of the ethyl group (affording the C_s symmetric "syn" rotamer **4b** (not shown), 1.5 kcal/mol higher in energy) and subsequent loss of one bridging hydrogen and one terminal hydrogen (**TS4b/5**) with an activation barrier of 40.2 kcal/mol relative to **4**. The transition state is quite late as judged by the long departing B- -H distances in **TS4b/5** (1.919 and 2.031 Å) as well as the small reverse activation barrier (5.5 kcal/mol). The resulting Et−B_4H_7 isomer **5** is also an intermediate on path II (see below) and can rearrange to the basket compound **1** with a small barrier (**TS5/1**).

On the potential energy surface, Et−B_4H_9 isomer **4** is 6.3 kcal/mol lower in energy than **1** + H_2. Entropy favors the latter products which become slightly more stable at higher temperatures (Table 1). The driving force is small, however, and the barrier for H_2 elimination from **4** is large, so that an appreciable fraction of **4** should be detected if all or part of **1** would be produced via path I.

On the other hand, it is reasonable to assume that Et−B_4H_9 isomers such as **4**, once formed, can further react with ethene

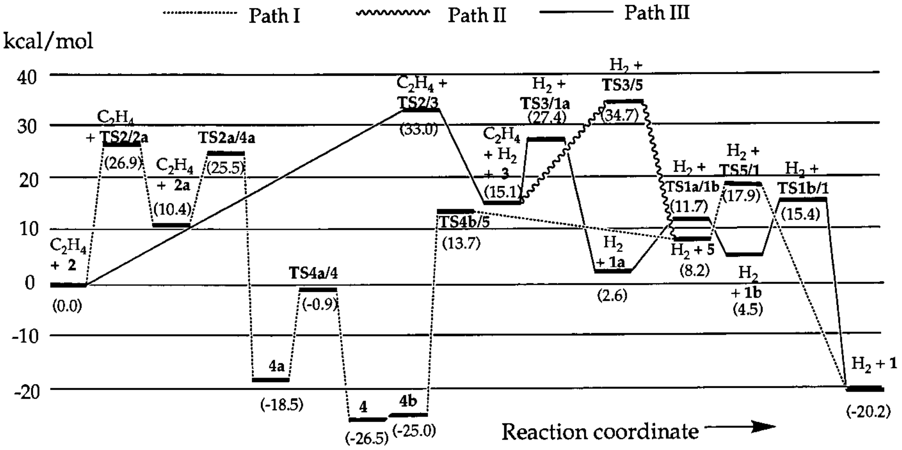

Figure 4. Schematic reaction profile for paths I–III. The [MP4/b] + ZPE values from Table 1 are plotted relative to **2** + C_2H_4.

present in the mixture to afford cage-substituted basket derivatives such as Et–$(CH_2CH_2)B_4H_7$. The latter compound must have the ethyl group in the exo position with respect to the B_4 "butterfly" moiety, whereas in **4** the ethyl group is in the endo position. In fact, isomer **4c** with an *exo*-ethyl group ("anti-rotamer" in C_s symmetry, not shown) is computed to be 1.2 kcal/mol more stable than **4**. This exo-isomer can react with C_2H_4 to form an ethyl-substituted version of **1** via, e.g. a route analoguous to path III (see below). Since our main focus is the formation of **1** and not this hydroboration side reaction, we have not computed the complete pathway leading to **4c** and further to Et–$(CH_2CH_2)B_4H_7$. The overall energetics are probably similar to those discussed above (and below).

Indirect Hydroboration (Path II). The chemical evidence mentioned in the Introduction, together with the results for path I discussed above, suggest that H_2 is lost before the olefin is added and that B_4H_8 (**3**) is initially formed. A true transition state was located for an ethene molecule approaching **3** from the concave side (**TS3/5**, Figure 2) where one B–C bond is formed under simultaneous transfer of one H atom to the other C atom. Intermediate **5** (already discussed in connection with path I) thus results from hydroboration of C_2H_4 by **3**. Note that, in this case, the B atom forming the B–C bond does not provide the H atom transferred to the olefin. This H atom can be "returned" to the B_4 cage under simultaneous formation of the second B–C bond (**TS5/1**), affording the basket, **1**. This second step has a lower activation barrier and is more exothermic than the first one (Table 1). Hence, formation of **5** is the critical step in this sequence. The overall barrier relative to **2** + C_2H_4 is 34.7 kcal/mol, only slightly higher than that for formation of **3**, 33.0 kcal/mol (Table 1). Entropic effects increase this difference considerably, with computed $\Delta G^{\ddagger}$(373 K) values of 39.4 and 32.1 kcal/mol, respectively, suggesting that formation of **5** should be the rate-determining step for this route.

The fact that the **2** + C_2D_4 reaction product has all deuterons retained in the handle, however, argues strongly against path II. The corresponding intermediate $CD_2HCD_2–B_4H_7$ (d_4-**5**) should not only produce $(CD_2CD_2)B_4H_8$, but also $(CDHCD_2)B_4DH_7$ (in an approximate ratio of 1:2), provided the barrier for Me group rotation in **5** is much lower than that for basket formation. The corresponding transition state (not shown) has been located, and the rotational barrier is indeed found to be very small (2.3 kcal/mol at the MP2/6-31G(d) + ZPC level). Thus, the main path cannot involve **5**, and ethene must add directly to **3** without intermediate hydroboration.

Addition (Path III). Direct addition with simultaneous formation of both B–C bonds can be enforced computationally by imposing symmetry. A corresponding stationary point in C_{2v} symmetry (**TS3/1**, Figure 3) turned out to be a true transition state at the MP2/6-31G(d) level. If C_{2v} symmetry were maintained all along the reaction path, the quadruply bridged form of B_4H_8 would be the reactant. Since the latter is not a minimum at that level,[4] a bifurcation must occur at some point between C_1-symmetric **3** + C_2H_4 and **TS3/1**.

Direct addition via **TS3/1** is computed to be much more unfavorable than the indirect hydroboration path II (via **TS3/5** and **5**). The barrier for the former process is 4.8 kcal/mol higher than that for the latter (Table 1). Since path II is not the main route, addition via **TS3/1** can be excluded based on these energetic grounds. Another path must therefore exist with a lower activation barrier, probably involving one or more intermediates without ethyl groups.

Since several Lewis adducts B_4H_8L are known, some of which have been structurally characterized;[29] a possible candidate for such an intermediate would be the $B_4H_8(C_2H_4)$ adduct **1a.** Indeed, **1a** is a minimum 12.5 kcal/mol below **3** + C_2H_4, from which it can be formed with an activation barrier of 12.3 kcal/mol (**TS3/1a**). Enthalpic and entropic contributions diminish the exothermicity and increase the barrier for this reaction, but the barrier remains always below that for formation of **3**, eq 2a. Thus, **1a** may indeed be a viable intermediate.

At the MP2/6-31G(d) + ZPC level, the association energy of **3** and C_2H_4 to form **1a** is −17.9 kcal/mol, significantly smaller than those computed at comparable levels for other Lewis adducts, for instance involving CO (−22.8 kcal/mol)[30] or PF_3 (−23.2 kcal/mol).[29b] For the latter adducts, the corresponding exo isomers (ligand and terminal H atom on hinge boron exchanged) were found to be only slightly higher in energy, between 0.6 (B_4H_8CO)[30] and 2.2 kcal/mol ($B_4H_8PF_3$);[29b] the same is found for *exo*-$B_4H_8(C_2H_4)$ (not shown), which is computed 1.7 kcal/mol above **1a** at the same level.

No transition state for direct rearrangement of **1a** to **1** could be located. Every attempt to close the contact between one C atom and the nearest wing-tip B atom resulted in the opening

---

(29) E.g.: (a) B_4H_8CO: Cranson, S. J.; Davies, P. M.; Greatrex, R.; Rankin, D. W. H.; Robertson, H. E. *J. Chem. Soc., Dalton Trans.* **1990**, 101. (b) $B_4H_8PF_3$: Brain, P. T.; Rankin, D. W. H.; Robertson, H. E.; Fox, M. A.; Greatrex, R.; Nikrahi, A.; Bühl, M. *Inorg. Chem.* **1997**, *36*, 1048. (c) $B_4H_8(PF_2NMe_2)$: LaPrade, M. D.; Nordman, C. E. *Inorg. Chem.* **1969**, *8*, 1669.

(30) Bühl, M.; Schleyer, P. v. R. *Struct. Chem.* **1993**, *4*, 1.

(31) The implicit assumption made here is that the formation of **4a** constitutes the main "entry channel" to these side products and that the barriers for all subsequent reactions leading to them are lower in energy than **TS2a/4a**.

of the adjacent B−B edge. Eventually we located **TS1a/1b** (9.1 kcal/mol barrier relative to **1a**) leading to a minimum **1b**, 1.9 kcal/mol above **1a** (Figure 3).

1b, which can be described as a nonclassical B_3H_7 molecule with a terminal $-CH_2CH_2BH_2$ group, can rearrange to **1** with a barrier of 11.0 kcal/mol (**TS1b/1**) and a driving force of 24.7 kcal/mol with respect to **1b**. This transition state bears a close resemblance to the one located[4a] in the reaction $B_4H_{10} \rightarrow B_3H_7 + BH_3$. In **TS1b/1** the CH_2CH_2 groups links the BH_3 moeity to the B_3H_7 moiety but does not otherwise significantly perturb the transition state structure. The vacant p orbital on the tethered BH_2 interacts with a bridging hydrogen in the substituted B_3H_7 while at the same time a terminal hydrogen of the BH_2 group begins to form a bridging interaction (Figure 3).

Along path III the barrier for each subsequent step is smaller than that for the preceding one. The only exception is the barrier from **1b** to **1** which is 3.7 kcal/mol larger than the barrier from **1b** back to **1a**. However, in this case, the energy difference between **1b** and **1a** is small and it is likely that an equilibrium is established. Thus, the reaction should proceed smoothly once the barrier for the initial B_4H_8 formation (eq 1) is overcome. The energetic barrier computed for this rate-determining process, however, is much higher than for any step involved in path I (compare relative energies of **TS2/3** + C_2H_4 and, e.g., **TS2/2a** + C_2H_4 or **TS2a/4a** in Table 1). Inclusion of entropic corrections, however, disfavor the hydroboration step in the latter and render path III lower in free energy; cf. the $\Delta G(373\ K)$ values for **TS2a/4a** and **TS2/3** + C_2H_4, 35.3 and 32.1 kcal/mol, respectively (Table 1). Since no hydrogen transfers to the olefin moiety are involved, this path is also consistent with the absence of H/D scrambling in the C_2D_4 experiments. The calculations therefore strongly suggest that path III is the major route of basket-compound formation.

Competition among Paths I−III. The computed potential-energy changes along the reaction coordinates of each path (paths I−III) are illustrated in Figure 4. To what extent could the hydroboration paths I and II compete with the addition path III? From the preceding section it is apparent that entropic effects are decisive. For better comparison with experiment, ΔG values at 100 °C, a typical reaction temperature, are discussed below.

As already mentioned, path I would eventually afford Et−B_4H_9 which is expected to further react with ethene, producing ethyl-substituted derivatives of **1**. The rate-determining step for this process is indicated to be the hydroboration step, e.g. **2a** + $C_2H_4 \rightarrow$ **4a**. The rate-determining step for formation of **1** from **2** via path III should be the initial dissociation **2** → **3** + H_2 (eq 2a). Assuming that all molecules following the former route end up as ethyl-substituted baskets,[31] an estimate can be made for their expected fraction of the final product, based on the free energy difference between **TS2a/4a** and **TS2/3** at 373 K (Table 1). The former is higher than the latter by 3.2 kcal/mol, corresponding (at 100 °C) to 1.3% of ethyl-substituted baskets. The amount of 2-Et−2,4-$(CH_2CH_2)B_4H_7$ actually isolated is of the same order of magnitude, 3%.[15] Higher theoretical levels and in particular, a more detailed computational study of the side reactions may be needed for definite conclusions. Nevertheless, we consider the present results to be consistent with the proposal that the major fraction of alkyl-substituted basket side products arises from path I/path III sequences as illustrated in, e.g. eqs 4a and 5. This mechanism would also explain why the final basket compounds are inert toward olefins:[14] the 2,4-ethano bridge in **1** prevents the rearrangement to isomers such as **2a** which could act as hydroborating agents.

Path II could be excluded because H/D scrambling should occur with C_2D_4 as reactant, which is not observed experimentally.[11] As mentioned in the Introduction, traces of H/D exchanged products might have gone unnoticed. Estimates for the expected fraction of such products, i.e., the ratio between molecules following path II and path III, can now be made on the basis of the free energy difference between **TS3/5** and **TS3/1a**. At 100 °C, the corresponding $\Delta G^{\ddagger}$ difference is nearly 12 kcal/mol (Table 1), from which a fraction of H/D exchanged product of no more than 0.1 ppm could be expected. Thus, path II can indeed be fully excluded.

Conclusions

Three pathways leading from B_4H_{10} (**2**) + C_2H_4 to the basket compound $(CH_2CH_2)B_4H_8$ (**1**) + H_2 have been studied computationally. The preferred mechanism involves H_2 dissociation from **2** (as rate-determining step) and consecutive formation of two intermediates, first, a $B_4H_8(C_2H_4)$ adduct (**1a**) and, second, a $-CH_2CH_2BH_2$ substituted B_3H_7 isomer **1b** (path III). Of the two alternative pathways involving ethene hydroboration, that using B_4H_8 (**3**) as hydroborating agent (path II) is too high in energy and can be excluded. Path I involving a B_4H_{10} isomer (**2a**) as hydroborating agent, however, can be competitive; in fact, this would be the most favorable route as far as potential energies (or enthalpies) are concerned. Entropy effects disfavor the hydroboration step to such an extent that path III is the main route under the experimental conditions. The primary product of path I, Et−B_4H_9 (**4**), is quite stable with respect to **1** + H_2 (which are favored entropically only at higher temperatures), precluding efficient formation of **1** via this route. It is rather suggested that **4** or isomers thereof can take up another ethene molecule via a route analoguous to path III, eventually leading to ethyl-substituted derivatives of **1**. Such derivatives are indeed observed as side products, in yields compatible with the activation barriers computed for the two branches.

In borane chemistry, even seemingly simple reactions can have quite complicated pathways. This study is a further illustration how theoretical computations can unravel mechanistic details which are difficult or impossible to detect otherwise.

Acknowledgment. Computer time was provided by the Alabama Supercomputer Network, by the ETH Zürich (C4 cluster), and by the Swiss Center for Scientific Computing in Manno, Switzerland. M.B. wishes to thank W. Thiel for his continuous support. M.L.M. thanks Sun Microsystems Computer Corp. for the award of an Academic Equipment Grant.

Supporting Information Available: Absolute and zero-point energies of all species are collected in (Table S1) and Cartesian coordinates for relevant structures optimized at the MP2/6-31G(d) (Table S2) (10 pages). Ordering information is given on any current masthead page.

IC980352V